Since January 2020 Elsevier has created a COVID-19 resource centre with free information in English and Mandarin on the novel coronavirus COVID-19. The COVID-19 resource centre is hosted on Elsevier Connect, the company's public news and information website.

Cell Host & Microbe
Article

Nonsense-Mediated Decay Serves as a General Viral Restriction Mechanism in Plants

Damien Garcia,[1,*] Shahinez Garcia,[1] and Olivier Voinnet[1,2,*]
[1]Institut de Biologie Moléculaire des Plantes (IBMP), Centre National de la Recherche Scientifique, UPR 2357, 67084 Strasbourg, France
[2]Swiss Federal Institute of Technology Zurich, Department of Biology, Universitätstrasse 2, 8092 Zürich, Switzerland
*Correspondence: damien.garcia@ibmp-cnrs.unistra.fr (D.G.), voinneto@ethz.ch (O.V.)
http://dx.doi.org/10.1016/j.chom.2014.08.001

SUMMARY

(+)strand RNA viruses have to overcome various points of restriction in the host to establish successful infection. In plants, this includes RNA silencing. To uncover additional bottlenecks to RNA virus infection, we genetically attenuated the impact of RNA silencing on transgenically expressed *Potato virus X* (PVX), a (+)strand RNA virus that replicates in *Arabidopsis*. A genetic screen in this sensitized background uncovered how nonsense-mediated decay (NMD), a host RNA quality control mechanism, recognizes and eliminates PVX RNAs with internal termination codons and long 3′ UTRs. NMD also operates in natural infection contexts, and while some viruses have evolved genome expression strategies to overcome this process altogether, the virulence of NMD-activating viruses entails their ability to directly suppress NMD or to promote an NMD-unfavorable cellular state. These principles of induction, evasion, and suppression define NMD as a general viral restriction mechanism in plants that also likely operates in animals.

INTRODUCTION

(+)strand RNA viruses account for important human diseases, such as severe acute respiratory syndrome or hepatitis C, and comprise most arthropod-borne viruses, including Dengue and yellow fever viruses. They also encompass the majority of plant viruses, accounting for substantial losses in crop yields worldwide. Experimental systems developed in plants, invertebrates, and mammals have jointly contributed to define major aspects of (+)strand RNA virus biology. Typically, the viral genomic (g) RNA is first uncoated and translated to produce the replicase required for (−)strand RNA synthesis via double-stranded (ds) RNA replication intermediates (RIs). The (−)strand is then a template for synthesis, in 10- to 100-fold excess, of (+)strand RNAs subsequently replicated, translated, or packaged into virions. For many viruses with polycistronic gRNAs, the (−)strand also supports transcription of one or several 3′-coterminal subgenomic (sg)RNAs translated into various viral products. At nearly all these steps, viruses require host compatibility factors and simultaneously face host restriction pathways that they must suppress or evade to retain virulence (Nagy and Pogany, 2012).

In plants, a highly specific adaptive immunity to viruses and other microbes relies on evolving repertoires of disease resistance (R) proteins that recognize pathogen-encoded protein variants. R protein activation by a matching viral product induces defense reactions culminating in programmed cell death and systemic release of defense-related hormones (Soosaar et al., 2005). Besides this adaptive immunity, intrinsic RNA-based virus restriction pathways exist in plants, among which RNA silencing has been the main focus of attention so far, owing to its activation by viruses in plants but also across kingdoms (Ding and Voinnet, 2007). In RNA silencing, viral dsRNA RIs are processed into 21–24 nt small interfering (si)RNAs by RNase III enzymes in the Dicer-like (DCL) family. Incorporated into ARGONAUTE (AGO)-containing protein complexes, siRNAs then guide sequence-specific silencing of complementary viral RNA. Endogenous RNA-dependent RNA polymerases (RDRs) may also use viral RNA for de novo dsRNA synthesis followed by secondary siRNA production that reinforces the host silencing response. So prevalent is this amplification mechanism in plants that it has hindered the genetic dissection of the primary antiviral silencing response: how, when, and where in the cell viral RNAs are initially accessed by the silencing machinery remain essentially unknown (Pumplin and Voinnet, 2013). Limited reverse genetics data implicate *Arabidopsis* DCL4 as a major antiviral Dicer alongside its surrogate, DCL2, while AGO1 and AGO2 are effectors of antiviral silencing; RDR6 and its paralog, RDR1, account for the production of amplified siRNAs during virus infections (Pumplin and Voinnet, 2013).

Attempts to dissect plant virus compatibility and restriction by forward genetics have been hampered by the tediousness and inconsistency of large-scale virus inoculation procedures. A solution has been to package viruses into plant cells under the form of transgenes called "amplicons," as decribed for the (+)strand RNA virus *Potato virus X* modified to express the green fluorescent protein: PVX-GFP (Dalmay et al., 2000a). Because *Arabidopsis* is not a host for PVX, it was anticipated to accommodate low replication levels not detrimental to plant development. However, PVX-GFP accumulation in transgenic lines was strongly suppressed owing to robust and consistent RNA silencing (Dalmay et al., 2000a). One avatar of the PVX-GFP amplicon involved its coexpression with a separate GFP transgene

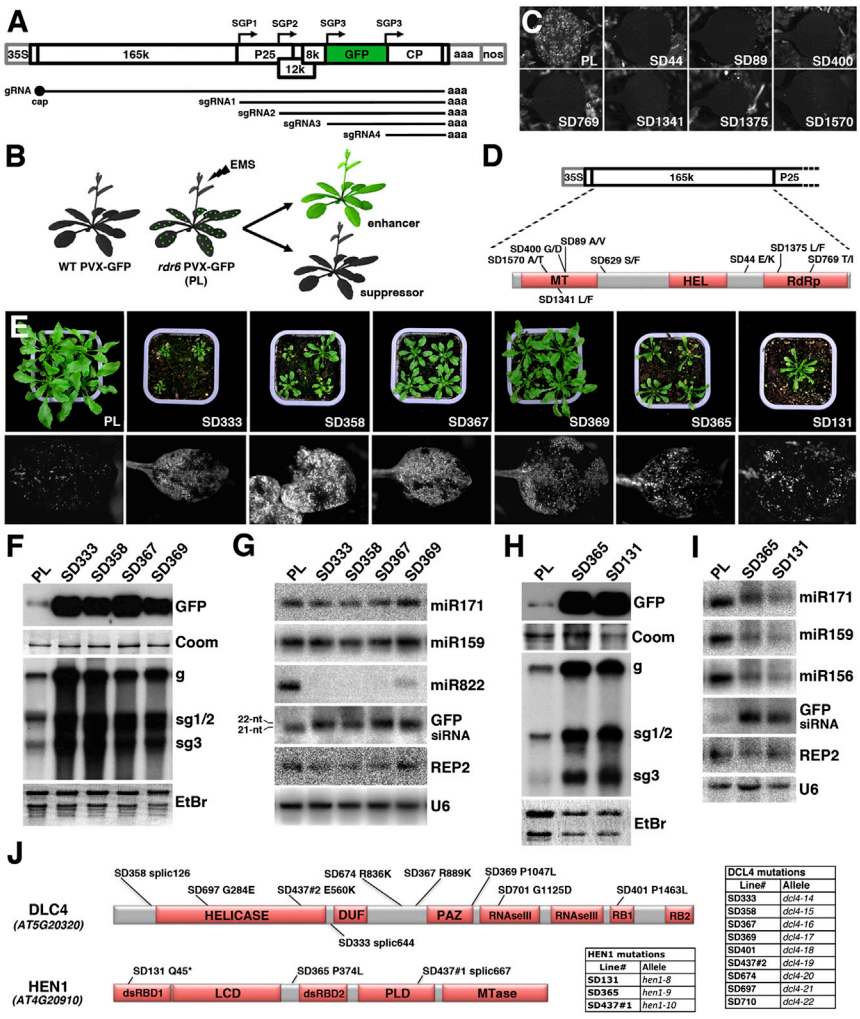

Figure 1. A Sensitized Genetic Screen for PVX-GFP Modifiers in *Arabidopsis*

(A) Structure and expression strategy of the PVX-GFP genome in the context of the expression vector used in this study. 35S: *Cauliflower mosaic virus* 35S promoter; Nos: nopaline synthase terminator; aaa: poly $(A)_{12}$ tract. CP: coat protein; P25, 12k, 8k: triple-gene block for movement proteins. 165k: replicase; gRNA: genomic RNA; sgRNA: subgenomic RNA; SGP: sgRNA promoter.

(B) Strategy of the PVX-GFP modifier screen in the *rdr6* parental line (PL).

(C) Cotyledons of PVX-GFP intragenic suppressors under UV illumination 13 days postgermination (dpg).

(D) Mutations identified in the viral replicase ORF in the lines depicted in (C). Conserved domains are indicated by red boxes and amino acid transitions (X/Y) are shown. MT: guanylyltransferase/methyltransferase-like; HEL: RNA helicase-like; RdRp: RNA-dependent RNA polymerase.

(E) Selected PVX-GFP enhancer lines. Pictures of whole plants and individual leaves were taken 21 dpg under visible (top) and UV (bottom) light.

(F) Western and northern analyses of GFP and PVX-GFP in seedlings of the indicated lines 21 dpg.

(G) Northern analysis of endogenous and PVX-GFP-derived small RNAs in the samples analyzed in (F).

(H) Same as in (F) but in whole inflorescences of the indicated lines.

(I) Northern analysis of endogenous and PVX-GFP-derived small RNAs in lines analyzed in (H).

(J) Mutations identified in DCL4 and HEN1. DUF: domain of unknown function; PAZ: PIWI ARGONAUTE ZWILLE; RB1/2: dsRNA binding domain 1/2; LCD: La-motif-containing domain; PLD: PPIase-like domain; MTase: methyltransferase; Coom: Coomassie staining of total proteins; EtBr: Ethidium bromide staining of total RNA; U6: U6 small RNA; sg1/2/3: PVX-GFP sgRNAs1/2/3. See also Figure S1 and Tables S1 and S2.

acting as a silencing amplifier device (Dalmay et al., 2000a). This system was used in a forward genetic screen for *silencing deficient* mutants (*sde*), which was biased toward the identification of silencing amplification/maintenance components, including SDE1 (later renamed RDR6) and the RNA helicase and RDR6 cofactor, SDE3; of note, none of the primary antiviral silencing components evoked above was retrieved in this or, indeed, other amplicon-based screens (Dalmay et al., 2000b, 2001; Herr et al., 2005).

The *Arabidopsis* PVX-GFP amplicon alone, without the second GFP transgene, is also restricted by the action of RDR6 and SDE3: mutations in either component restore PVX-GFP accumulation manifested by sporadic GFP lesions (Garcia et al., 2012). We reasoned that *rdr6* PVX-GFP *Arabidopsis*, being viable and fertile, could be used in forward genetics to identify enhancers and suppressors of this moderate green fluorescent phenotype. Suppressors would likely define the still-elusive host-encoded compatibility factors required for PVX replication. Enhancers would possibly encompass thus far inaccessible primary silencing components or hitherto undiscovered viral restriction pathways unrelated to silencing. The outcome of this sensitized genetic screen, disclosed here, concurs with these predictions and uncovers NMD as an intrinsic restriction pathway for (+) strand RNA viruses.

RESULTS

Enhancers and Suppressors of PVX-GFP in *Arabidopsis*

UV-coupled binoculars were used to screen the progeny of a population of ~5,000 EMS-mutagenized *rdr6* PVX-GFP plants defining the parental line (PL). We scored accumulation of GFP produced from the viral sgRNA3 via a duplicated coat protein (CP) promoter (Figure 1A). Fifty-one enhancers and 13 suppressors were recovered at the seedling stage, displaying higher and lower green fluorescence, respectively (Figure 1B). Strikingly, eight suppressors had intragenic mutations within the PVX 165k replicase open reading frame (ORF), often affected in conserved domains (Figures 1C and 1D). Accordingly, these lines accumulated low PVX-GFP levels (Figures S1A and S1B), and crude virion sap extracts prepared from most of them were not infectious in *Nicotiana clevelandii* (Figures S1C and S1D). The PL is thus amenable to the genetic exploration of virus

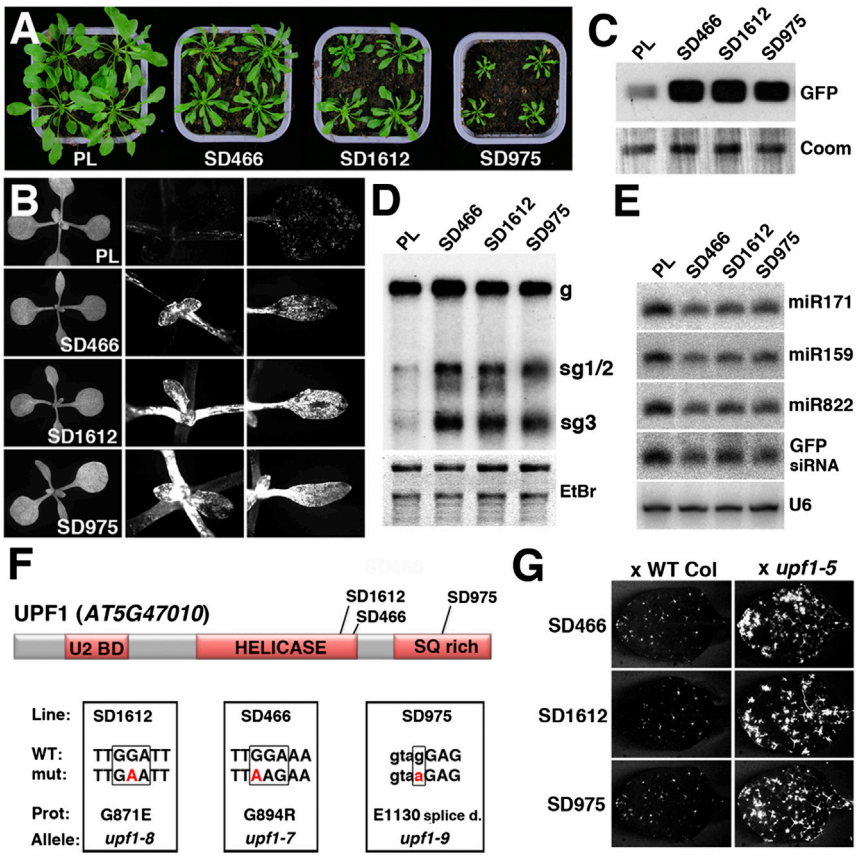

Figure 2. Mutations in *UPF1* Enhance PVX-GFP Levels

(A) Morphological defects in three PVX-GFP enhancer lines at 42 dpg.

(B) Lines shown in (A) under UV illumination at 18 dpg. First row: plant morphology revealed by chlorophyll autofluorescence; second and third rows: GFP fluorescence in emerging leaves and primordia.

(C and D) Western and northern analyses of GFP and PVX-GFP at 21 dpg.

(E) Northern analysis of endogenous miRNAs and viral siRNAs at 21 dpg.

(F) Mutations in *UPF1* identified in SD466, SD1612, and SD975.

(G) GFP accumulation in F1 plants from a cross between PVX enhancers and WT or *upf1-5*. U2 BD: UPF2 binding domain; Helicase: RNA helicase domain; splice d.: splicing defect.

replication, suggesting that some of the remaining extragenic suppressors affect basic PVX compatibility factors.

Extragenic enhancers likely affected PVX restriction factors, including primary antiviral silencing effectors presumably poorly accessible in RDR6-proficient plants. Lines SD333, SD358, SD367, and SD369 defined a first enhancer group displaying increased GFP accumulation and higher levels of PVX-GFP RNAs, likely accounting for their reduced stature and fertility (Figures 1E and 1F). The four mutants displayed normal levels of DCL1-dependent miRNAs and of the DCL3-dependent heterochromatic small (s)RNA REP2; by contrast, the DCL4-dependent miR822 was below detection (Figure 1G). PVX-GFP-derived siRNAs, 21 nt in length in the PL, migrated as 22 nt species in the mutants, a diagnostic of DCL2 surrogate antiviral activity (Figure 1G) (Deleris et al., 2006). The four mutations mapped on the chromosome V upper arm in a region containing *DCL4*, in which all four lines displayed mutations (Figure 1J and Table S1). This was also the case of six additional enhancers retrieved later based on similar GFP and sRNA phenotypes (Figure S1E and Table S1). Noncomplementation of five of these mutants upon crosses with *dcl4-2* confirmed that this first enhancer class defines an extensive series of *dcl4* alleles, renamed *dcl4-14* to *dcl4-22* (Figures 1J and S1F–S1J and Table S1).

The enhancer lines SD365 and SD131 had a stunted growth and increased GFP and PVX-GFP RNA levels relative to the PL (Figures 1E and 1H). Unlike the *dcl4* enhancers, however, they showed an upward leaf curling typical of miRNA-deficient mutants (Figure 1E). These lines indeed had low levels of mature miRNAs, but also of the heterochromatic sRNA REP2, with both sRNA species appearing as smears in northern blot (Figure 1I). This was reminiscent of mutations in *HUA ENHANCER 1* (*HEN1*) required for 2′ O-methylation of endogenous and viral sRNAs, which protects them from uridylation and degradation (Li et al., 2005). Two of these mutations were mapped on chromosome 4 between markers UPSC_4-41152 and ciw7, an interval containing *HEN1*. Genomic sequencing confirmed that SD365, SD131, and SD437#1, an additional mutant with similar defects, carry EMS-induced lesions in *HEN1* (Figure 1J and Table S2). Moreover, all lines showed noncomplementation with *hen1-6* and were accordingly renamed *hen1-8* to *hen1-10* (Figures S1K, S1L, and 1J and Table S2). DCL4 and HEN1 are known to, respectively, produce and protect virus-derived siRNAs (Boutet et al., 2003; Deleris et al., 2006), providing a proof of principle that the *rdr6*-sensitized background is amenable to the investigation of primary antiviral silencing.

Nonsense-Mediated Decay Suppresses the PVX-GFP Amplicon

Lines SD466, SD1612, and SD975 defined a third class of enhancers. These exhibited a distinctive narrow leaf phenotype and stronger green fluorescence predominantly in new emerging leaves and primordia (Figures 2A and 2B), which, accordingly, contained significantly higher viral GFP levels than in the PL (Figure 2C). However, northern analyses employing a GFP probe showed that, unlike in the *dcl4* and *hen1* enhancers, the levels of viral gRNA remained nearly the same as in the PL (Figure 2D). By contrast, those of the sgRNA1/2 and sgRNA3, which produces the viral GFP, were significantly increased. The levels of PVX-GFP siRNAs and endogenous miRNAs/siRNAs tested were unchanged, suggesting that SD466, SD1612, and SD975 are silencing-unrelated mutants (Figure 2E). The three mutations mapped on chromosome 5 within a 350 kb interval delineated by markers MZA15-1 and MNJ7-1, containing the gene encoding

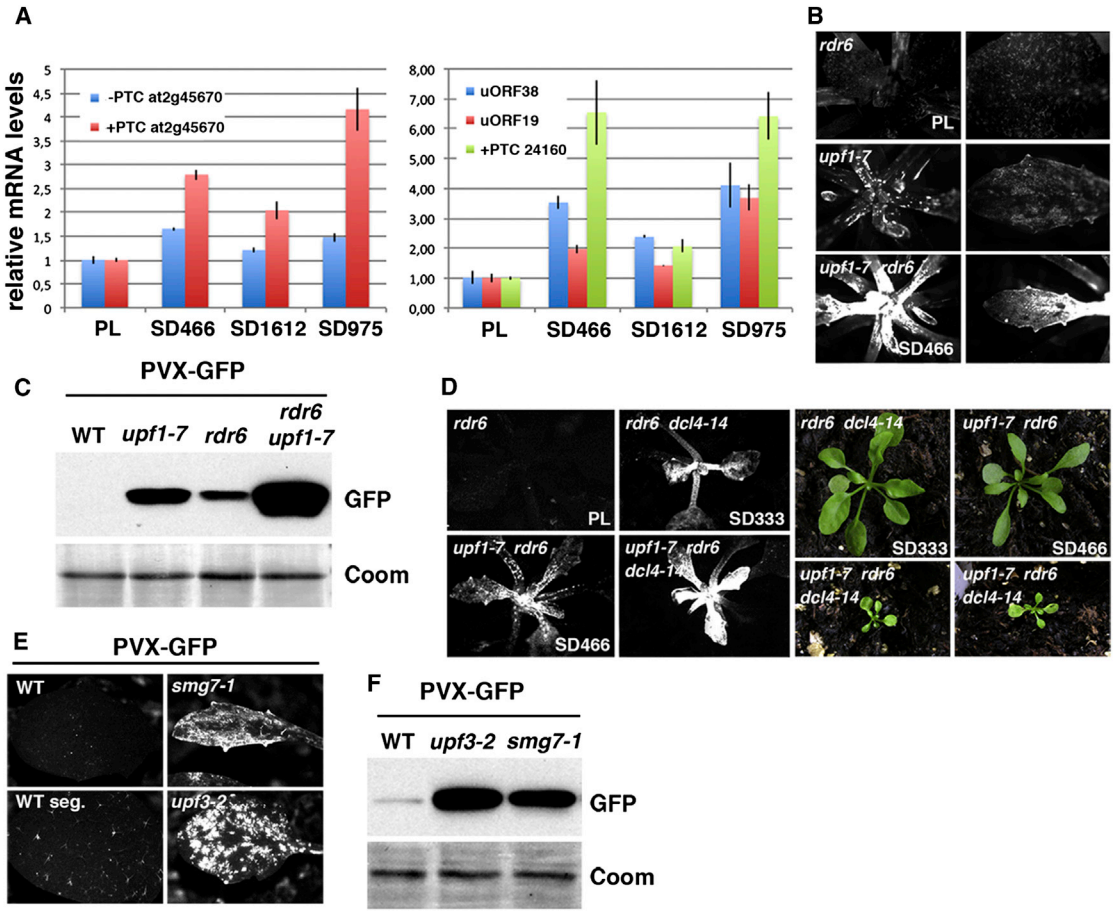

Figure 3. *upf1* and Other NMD Mutants Increase PVX-GFP and Endogenous NMD Target Levels

(A) Quantitative PCR (qPCR) analysis of known NMD target transcripts containing premature termination codons (PTC) or upstream ORFs (uORFs) in SD466, SD1612, and SD975, normalized to Actin2 and presented as mean ± SEM.

(B) UV illumination of leaves showing the effect on PVX-GFP levels of *upf1*-7 alone or in combination with *rdr6*.

(C) Western analysis of GFP levels in the plants shown in (B).

(D) Cumulated effect of mutations in *UPF1*, *RDR6*, and *DCL4* on PVX-GFP levels and plant morphology.

(E) Picture under UV light of the *smg7-1* and *upf3*-2 mutants, introgressed into the PVX-GFP background.

(F) Western analysis of GFP levels as in (E).

the RNA helicase Up-Frameshift 1 (UPF1), whose inactivation causes a narrow leaf phenotype in *Arabidopsis* (Riehs-Kearnan et al., 2012). Genomic sequencing revealed that SD466 and SD1612 harbor mutations in the *UPF1* ATPase domain, while a lesion in the C-terminal SQ-rich domain is predicted to disrupt splicing of *UPF1* in SD975 (Figure 2F). Noncomplementation upon crosses with *upf1-5* confirmed that SD466, SD1612, and SD975 define unique alleles of *UPF1*, renamed *upf1-7*, *upf1-8*, and *upf1-9* (Figures 2F and 2G).

UPF1 is the core effector of NMD, a paneukaryotic RNA quality control pathway that prevents expression of mRNAs containing premature termination codons (PTCs) with the potential, therefore, to produce truncated, harmful proteins (Kervestin and Jacobson, 2012). In yeast, metazoans, and plants, NMD promotes accelerated mRNA decay in cytoplasmic processing bodies (P-bodies) and may also affect protein production (Isken et al., 2008; Muhlrad and Parker, 1999). While these mRNA-targeting steps are less well characterized in plants, orthologs of key NMD components are found in *Arabidopsis*, including UPF1, its core cofactors UPF2 and UPF3, as well as SMG7, which recruits phosphorylated UPF1 to P-bodies (Kerényi et al., 2008). Accordingly, *Arabidopsis* mutants available in this pathway, *upf1*, *upf3*, and *smg7*, overaccumulate endogenous RNAs with known NMD-activating features. These include mRNAs containing upstream ORFs (uORFs) that create unusually long 3′ untranslated regions (3′ UTRs), mRNA-like noncoding RNAs, and PTC-containing mRNA variants produced by alternative splicing. Several such validated NMD targets displayed significantly increased levels in SD466, SD1612, and SD975 (Figure 3A) (Rayson et al., 2012; Riehs-Kearnan et al., 2012). This suggested that the host NMD machinery might also target PVX-GFP-derived RNA species, although confounding/cumulative effects of the *rdr6* background could not be ruled out at this stage.

We thus outcrossed *rdr6* in SD466, enabling a comparison of viral GFP levels between *upf1-7*, *rdr6*, and *upf1-7 rdr6*

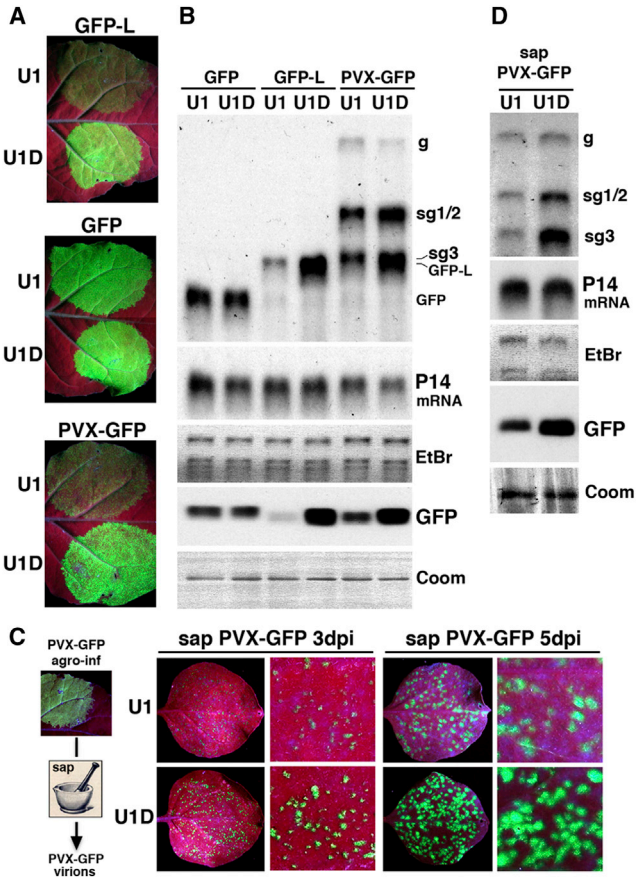

Figure 4. NMD Restricts PVX-GFP in Authentic Infection

(A) UV illumination of *N. benthamiana* leaves coagroinfiltrated with wild-type (U1) or dominant-negative (U1D) versions of UPF1 together with the P14 silencing suppressor and the constructs indicated, at 3 dpi.

(B) Northern (higher panel) and western (lower panel) analyses of GFP and PVX-GFP levels in the tissues depicted in (A).

(C) UV illumination, at 3 and 5 dpi, of PVX-GFP sap inoculation of *N. benthamiana* leaves preinfiltrated 1 day earlier with P14 and either U1 or U1D.

(D) Viral RNA and GFP accumulation in leaves shown in (C) at 3 dpi.

(Figure 3B). In a segregating F2 population, *upf1-7* alone was sufficient to derepress viral GFP accumulation at a higher level than *rdr6* (Figures 3B and 3C). In plants combining *rdr6* and *upf1-7*, the viral GFP levels were higher than in each individual mutant and even exceeded those expected from their additive effects (Figures 3B and 3C). This was also manifested if primary silencing mediated by DCL4 was compromised: crossing the SD333 enhancer (*dcl4-14 rdr6*, Figure 1E) with SD466 (*upf1-7 rdr6*) resulted in a segregating F2 population in which *upf1-7 dcl4-14 rdr6* mutants consistently exhibited stronger green fluorescence than either of their parents (Figure 3D); molecular analyses were precluded by extreme dwarfism and rapid death presumably caused by PVX-GFP overload (Figure 3D). Therefore, RNA silencing and UPF1 define nonepistatic and possibly competing pathways that concurrently repress the PVX-GFP amplicon in both WT and *rdr6*. NMD underlies the effects of UPF1 because introgression of either *upf3-2* or *smg7-1* into the PL also enhanced the viral GFP levels in homozygous segregants with a WT *RDR6* background (Figures 3E and 3F).

NMD Restricts PVX-GFP in Natural Infection Contexts

Because *Arabidopsis* is not a PVX host, we could not use the amplicon system to address if, like RNA silencing, NMD restricts PVX infections naturally. The necessary transgenic nature and nuclear phases of amplicon expression could also have created artificial conditions favorable to NMD but not found in normal infections during which PVX RNA replication is exclusively cytoplasmic. To overcome these caveats, we exploited an existing NMD suppression assay based on Agrobacterium-mediated transient expression in *N. benthamiana*, a well-established PVX host. In this assay, a candidate NMD target is coexpressed with either a WT (U1) or dominant-negative version (U1D) of *Arabidopsis* UPF1 under conditions where RNA silencing, which normally strongly limits transient gene expression, is suppressed by the concomitant expression of the *Pothos latent virus* P14 protein (Kertész et al., 2006). As reported, an NMD-activating reporter GFP mRNA bearing a long 3′ UTR (GFP-L) was turned over 3 days after coinfiltration with construct U1, an effect suppressed if the UPF1-antogonistic construct, U1D, was used instead (Figures 4A and 4B) (Kertész et al., 2006). By contrast and also as reported, the GFP mRNA without a long 3′ UTR, and hence not targeted by NMD, accumulated to similarly high levels upon its coexpression with either the U1 or U1D construct (Figures 4A and 4B). In several independent experiments, GFP expression from PVX-GFP was low when it was coexpressed with U1, but high with U1D (Figures 4A and B). As in *Arabidopsis* SD466, SD1612, and SD975, the PVX-GFP gRNA levels remained nearly unchanged, while those of sgRNA1/2 and sgRNA3 were consistently higher in U1D- compared to U1-treated samples, as assessed using a GFP probe (Figures 2D and 4B).

We then adapted the above assay under conditions of authentic infections. A crude virion sap extract was prepared from PVX-GFP agro-inoculated tissues and rub-inoculated onto *N. benthamiana* leaves infiltrated 1 day earlier with either the U1 or U1D construct, in combination with P14 (Figure 4C). In several experiments, the density and fluorescence of primary PVX-GFP lesions were consistently higher in U1D- than in U1-treated leaves at both 3 and 5 days post-virus inoculation (dpi) (Figure 4C). Northern analyses employing a GFP probe revealed that the PVX-GFP gRNA levels were nearly unchanged in U1D- compared to U1-treated leaves at 3 dpi. Those of sgRNA1/2 and sgRNA3 were, by contrast, consistently higher in U1D-treated leaves, as were the viral GFP levels (Figure 4D). By 5 dpi, the PVX-GFP primary lesions had become confluent and reached the veins of U1D-treated leaves, whereas they were still individualized and less densely distributed in U1-treated leaves (Figure 4C). We conclude that NMD restricts PVX-GFP accumulation during authentic infections.

Extended 3′ UTRs in sgRNA1/2 and sgRNA3, but Not in sgRNA4, Account for Their Selective Targeting by NMD

The most-studied NMD-targeted mRNAs contain PTCs spawned by aberrant splicing or mutations (Kalyna et al., 2012). Nonetheless, NMD also regulates physiological mRNAs with a stop codon located in an environment unfavorable to

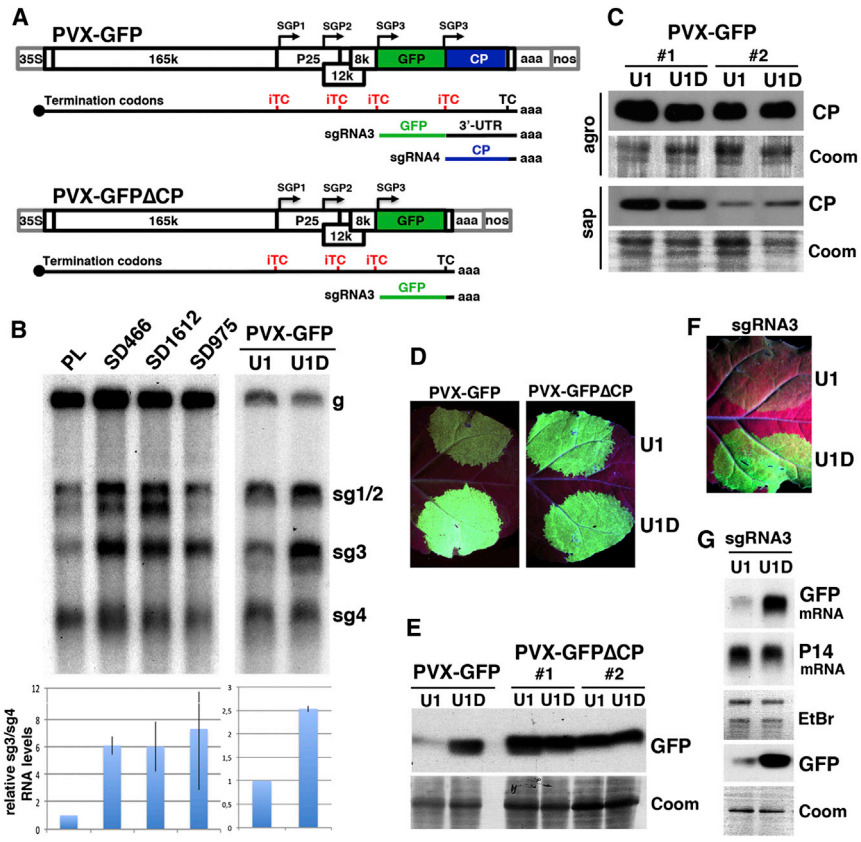

Figure 5. NMD Targets Viral RNA Containing Internal Premature Termination Codons

(A) PVX-GFP variants used in the experiments in (B)–(E).

(B) Northern blots from Figures 2E and 4B, hybridized with a CP probe. Signal quantification of relative sgRNA3/sgRNA4 ratios is shown in the lower panel. Error bars show mean ± SEM between two biological replicates.

(C) Higher panel: western analysis of CP levels in *N. benthamiana* leaves agroinfiltrated with PVX-GFP, P14, and either U1 or U1D, at 3 dpi. Lower panel: similar analysis but in sap-inoculated tissues at 7 dpi.

(D) NMD suppression assay conducted with PVX-GFP or PVX-GFPΔCP, observed under UV illumination at 3 dpi.

(E) Western analysis of GFP levels in the tissues shown in (D).

(F) NMD suppression assay conducted with sgRNA3 expressed from a binary vector.

(G) Northern and western analysis of GFP levels in the tissues in (F). iTC: internal termination codon; TC: termination codon.

translation termination. The plant NMD machinery, like its metazoan and yeast counterparts, uses at least two distinctive features to recognize such mRNAs, via separate mechanisms. The first mechanism is stimulated by the presence of introns within the 3′ UTRs of mRNAs; it specifically requires core components of the exon junction complex (EJC) deposited on mRNAs (Le Hir et al., 2001). A contribution of this mechanism to PVX-GFP suppression was highly unlikely since the PVX RNA genome is devoid of introns and replicated exclusively in the cytoplasm during natural infections. A second, EJC-independent NMD mechanism is triggered by mRNAs bearing unusually long 3′ UTRs (Kertész et al., 2006). The PVX-GFP genome contains several internal termination codons (iTCs) that create such extended 3′ UTRs in the full-length gRNA, sgRNA1/2, and sgRNA3 (Figures 1A and 5A). For instance, the CP-derived sequence bore by sgRNA3 defines an unusually long 3′ UTR for the GFP mRNA, a feature expected to stimulate NMD as with the GFP-L variant used in the transient assay (Figures 5A, 4A, and 4B). By contrast, sgRNA4, the most 3′-proximal in the PVX-GFP genome, contains the single CP ORF without a long 3′ UTR and should, therefore, evade NMD (Figure 5A). Because the same promoter drives them (Figure 5A), we thus compared the sgRNA3 and sgRNA4 steady-state and protein production levels in the context of active versus suppressed NMD.

To that aim, the RNA blots used in Figure 2D and Figure 4B were stripped and rehybridized with a CP- instead of the GFP-probe. In all cases, the sgRNA4 levels remained unchanged in UPF1-proficient compared to UPF1-deficient conditions, whereas, as expected, those of sgRNA3 and sgRNA1/2 were higher in UPF1-deficient conditions (Figure 5B). Furthermore, the sgRNA3/sgRNA4 ratio was up to 10-fold higher in the SD466, SD1612, and SD975 lines and also increased in U1D- compared to U1-treated leaves of PVX-GFP-infected *N. benthamiana* (Figure 5B). Thus, despite being transcribed from the same promoter, sgRNA4 is much less targeted by NMD than sgRNA3. Accordingly, the CP levels were unchanged in U1- compared to U1D-treated *N. benthamiana* leaves infected with PVX-GFP by sap inoculation or agroinfiltration (Figure 5C). The long 3′ UTR present in sgRNA3 but absent in sgRNA4 thus seemed to selectively stimulate NMD in the context of PVX-GFP, an idea further explored with PVX-GFPΔCP, which carries a deletion of the CP ORF dispensable for virus replication (Figure 5A). This modification concomitantly eliminates the long 3′ UTR of sgRNA3 and should accordingly cause the GFP mRNA to now evade NMD. Indeed, the GFP levels produced from PVX-GFPΔCP were equally high in U1- and U1D-treated *N. benthamiana* leaves, in stark contrast to the strong GFP increase seen with PVX-GFP in U1D- compared to U1-treated leaves (Figures 5D and 5E). The long 3′ UTR in sgRNA3 is not only necessary but also sufficient to trigger NMD because transient expression of sgRNA3 alone, under the 35S promoter, recapitulated all the effects observed in the PVX genome context (Figures 5F and 5G). Given that the P25 and 12k/8k ORFs are also followed by extended 3′ UTRs in sgRNA1 and sgRNA2 (Figures 1A and 5A), we infer that a similar NMD-activating mechanism accounts for the sensitivity of these two mRNAs to UPF1 activity, consistently observed under all experimental conditions (Figures 2D, 4B, and 4D). Therefore, the plant NMD machinery naturally discriminates and eliminates iTC- and long 3′ UTR-containing viral RNAs.

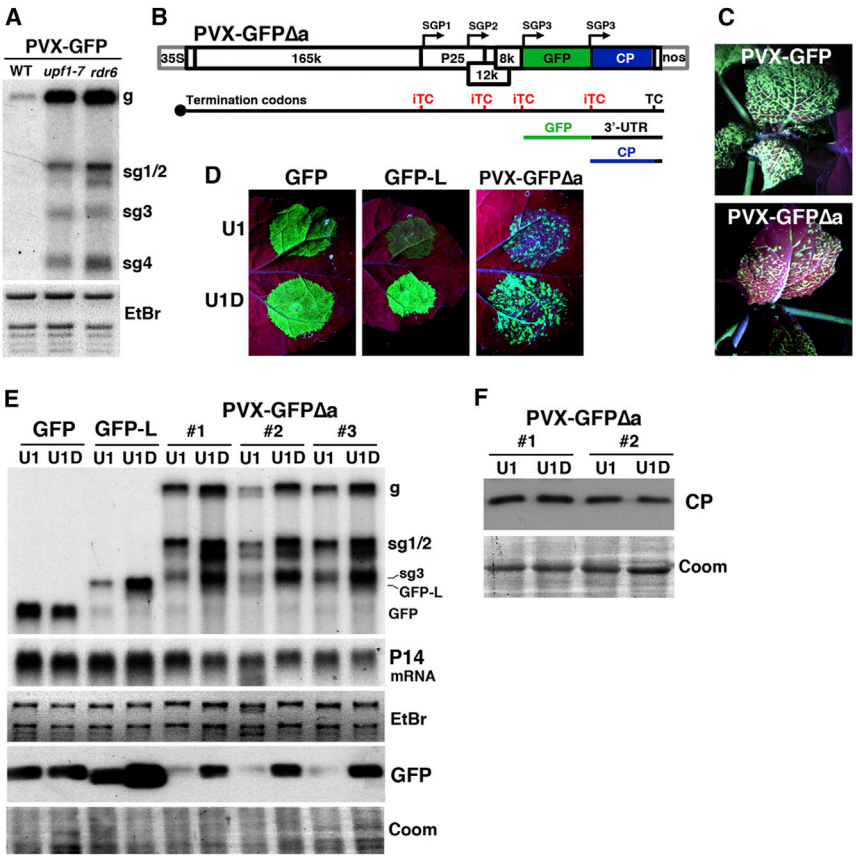

Figure 6. NMD Affects the PVX gRNA Early in Infection

(A) Northern analysis of PVX-GFP RNA levels in single *upf1* and *rdr6* mutants, using a CP probe.

(B) PVX-GFPΔa devoid of the 3′ end polyA stretch.

(C) Compared infectivity of PVX-GFPΔa and PVX-GFP in systemically infected *N. benthamiana* leaves at 7 dpi.

(D) NMD suppression assay conducted with PVX-GFP or PVX-GFPΔa, observed under UV illumination at 7 dpi.

(E) Northern (upper panel) and western (lower panel) analyses of viral GFP levels in tissues as in (D).

(F) Western analysis of CP levels in tissues as in (D).

NMD Also Targets the PVX-GFP gRNA under Conditions of Suboptimal Viral Replication/Accumulation

Unlike those of sgRNA1/2 and sgRNA3, the PVX-GFP gRNA levels remained largely unaltered by the suppression of NMD, both in *Arabidopsis* and *N. benthamiana* (Figures 2D, 4B, and 4D). This was intriguing since the 165k replicase ORF is followed by a 3′ UTR of 2.8 kb in the context of the translated gRNA (Figure 1A). Two interrelated features could have confounded a potential effect of NMD on the gRNA levels. First, sgRNAs are generally synthesized later than gRNAs during infection, as they encode late viral gene products; moreover, they are transcribed but not replicated and are not encapsidated. Comparatively, the gRNA is replicated as dsRNA very early during infection, and its accumulation reaches a plateau reflecting the packaging of novel gRNA copies into nuclease-resistant, inert virions (Hull, 2001). Thus, our analyses of steady-state as opposed to dynamic infection were possibly unsuited to appreciate a potential early impact of NMD on the PVX-GFP gRNA. Second, our studies were invariably conducted under conditions of RNA silencing suppression, caused either by the *rdr6* mutation in *Arabidopsis*, or by P14 in *N. benthamiana*. Yet, by sufficiently slowing down the early gRNA replication phase, active RNA silencing was perhaps required for the effects of NMD to be noticed. Indeed, in transgenic *Arabidopsis*, northern analyses with a CP probe showed that the PVX-GFP gRNA levels were strongly increased in the silencing-proficient *upf1-7* mutant; this increase was similar to that seen in *rdr6* (Figure 6A). Also as in *rdr6*, a strong gain in the levels of all sgRNAs was observed in *upf1-7* (Figure 6A), consistent with the transcription of sgRNA being initiated on viral (−)strands whose accumulation depends on gRNA abundance.

Conditions of active RNA silencing could not be employed in *N. benthamiana* because use of the P14 silencing suppressor is mandatory in the NMD assay. To create suboptimal virus replication conditions, we exploited previous observations that the infectivity of PVX in vitro transcripts lacking a 3′-polyA tail decreases considerably, as seen with polyA gRNAs of other viruses (Hemenway et al., 1990). We thus removed the 3′ end $(A)_{12}$ tract from PVX-GFP, creating the PVX-GFPΔa expression vector (Figure 6B). GFP was barely detectable 5 days after agroinoculation of PVX-GFPΔa, whereas it was readily visible in PVX-GFP-inoculated leaves; accordingly, systemic infection by PVX-GFPΔa was much less extensive than in PVX-GFP-inoculated plants, confirming the reduced infectivity of the modified virus (Figure 6C). In the NMD assay, the GFP levels from PVX-GFPΔa were significantly increased in U1D- compared to U1-treated leaves, indicating, as expected, that PVX-GFPΔa is NMD sensitive (Figures 6D and 6E). However, in contrast to the PVX-GFP gRNA levels, northern analyses with a GFP probe revealed a moderate yet consistent gain in PVX-GFPΔa gRNA levels in U1D- compared to U1-treated leaves (Figure 6E). As expected, the sgRNA1/2 and sgRNA3 levels were also increased under NMD-suppressive conditions, while those of the CP product of sgRNA4 remained unaltered (Figures 6E and 6F). Collectively, these results support the idea that NMD naturally targets the PVX gRNA during early phases of the infection in ways that are mostly evident under suboptimal virus replication conditions. Such conditions are naturally promoted by RNA silencing or may be created by artificially reducing PVX infectivity.

Induction and Evasion of NMD during Natural Infection by PVX-Unrelated Viruses

Many viruses phylogenetically unrelated to PVX produce mRNAs with long 3′ UTRs as a consequence of multiple iTCs. To address if NMD also targets such viruses, we used *Turnip crinkle virus*

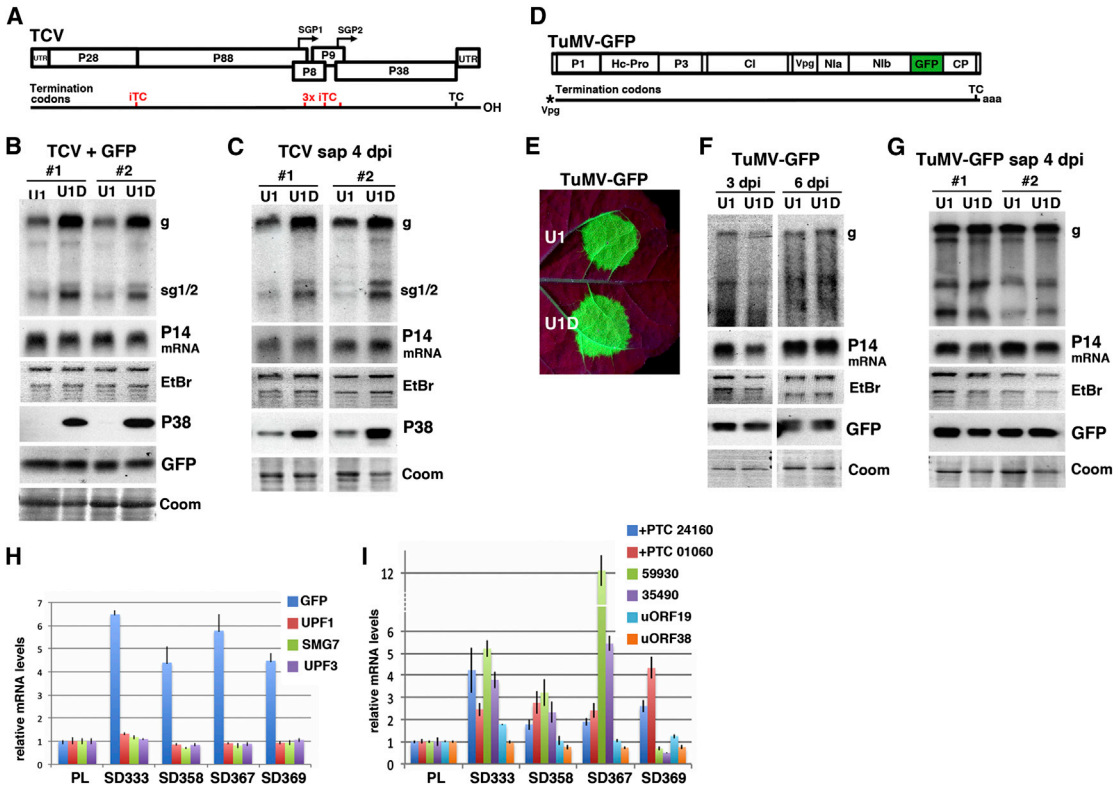

Figure 7. Induction, Evasion, and Suppression of NMD by Plant Viruses

(A) Genomic structure of TCV.

(B) Northern analysis of TCV RNAs and western analysis of P38 levels upon agroinfiltration of TCV with P14, GFP, and U1 or U1D, at 3 dpi.

(C) Northern and western analyses of *N. benthamiana* leaves infiltrated with P14 and either U1 or U1D and infected 1 day later with TCV sap.

(D) Genomic structure of TuMV-GFP.

(E) NMD suppression assay conducted with TuMV-GFP by agroinfiltration, observed under UV illumination at 6 dpi.

(F) Northern and western analyses of TuMV-GFP and GFP levels in tissues as depicted in (E), at 3 and 6 dpi.

(G) Northern and western analyses of *N. benthamiana* leaves infiltrated with P14 and either U1 or U1D and infected 1 day later with TuMV-GFP sap.

(H) qPCR analysis of viral GFP, UPF1, SM7, and UPF3 transcript levels in the *dcl4* mutants shown in Figure 1, at 21 dpi.

(I) qPCR analysis of *Arabidopsis* NMD target transcripts as in (H). qPCR in (H) and (I) were normalized to Actin2 and presented as mean ± SEM. See also Figure S2.

(TCV), a (+)strand RNA virus in the *Carmovirus* genus for which *N. benthamiana* is a host (Figure 7A). TCV produces two sgRNAs, sgRNA1 and sgRNA2, encoding proteins respectively involved in movement (P8, P9) and encapsidation/virulence (P38). In the gRNA context, the P88 replicase ORF is consequently followed by an extended 3′ UTR of 1.7 kb. Moreover, P88 is produced by readthrough translation of the most 5′-terminal ORF, P28, via suppression of an iTC defining, therefore, a bona fide PTC (Figure 7A). A strong NMD response was thus expected to target the TCV gRNA and to impact indirectly the accumulation of sgRNA1 and sgRNA2. This virus choice was also prompted by the lack of a 5′-cap and 3′-polyA tail in the TCV gRNA (Figure 7A), two characteristics of the PVX genome that may have influenced the onset of NMD. An infectious TCV clone was thus subjected to the NMD transient assay upon agroinoculation of *N. benthamiana* (Azevedo et al., 2010). In several independent experiments, the TCV gRNA accumulated to significantly higher levels in the U1D- compared to U1-treated samples, a difference also observed with the sgRNA levels and those of the sgRNA2 product, P38 (Figure 7B). By contrast, accumulation of GFP, produced from a coinfiltrated construct, used as a negative control, remained unchanged (Figure 7B). Similar results were obtained in several independent experiments involving authentic infections via a crude TCV virion sap extract (Figure 7C). Therefore, NMD is a general, virus-intrinsic restriction pathway activated independently of 5′ or 3′ end modifications of viral RNAs.

The constraints of NMD may have driven the emergence and selection of genome expression strategies allowing some viruses to evade this pathway. The (+)strand RNA potyviruses might provide an extreme illustration of this idea since the potyviral gRNA contains a single, large ORF translated as a ~350 kDa polyprotein precursor proteolytically processed into smaller products (Figure 7D). To test if, as anticipated, potyviruses evade NMD, we used an infectious cDNA clone of *Turnip mosaic virus* expressing GFP as a polyprotein-processing product (TuMV-GFP, Figure 7D). In several independent experiments, the GFP levels in TuMV-GFP agroinoculated leaves of *N. benthamiana* (a host of TuMV) were unchanged in the U1D- compared to U1-treated samples (Figures 7E and 7F). The viral gRNA levels were also unaltered, as assessed by northern analysis with a

GFP probe (Figure 7F). Near-identical results were obtained with natural infection using a TuMV-GFP virion sap extract (Figure 7G). The immunity of TuMV-GFP to NMD therefore suggests that the polyprotein strategy of potyviruses allows them to evade NMD by preventing iTC- and long 3′ UTR in viral RNAs.

Virulent PVX Infections Compromise Host NMD

While the above results illustrate how potyviruses evade NMD altogether, the virulence of NMD-activating viruses might be underpinned by their ability to suppress this mechanism. Many virulent plant viruses trigger RNA silencing and concurrently inhibit this process via dedicated suppressor proteins that often collaterally perturb host-silencing pathways (Pumplin and Voinnet, 2013). We reasoned that, similarly, viral suppression of NMD by virulent infections could be possibly diagnosed by a perturbation of endogenous NMD. We could not explore this idea in *N. benthamiana* since natural NMD targets have not yet been described in this genetically nonamenable species. We thus exploited the *Arabidopsis* PL, in which PVX-GFP accumulation and virulence are normally low (Figure 1B) but strongly enhanced in the *dcl4* mutant background, as in the SD333, SD358, SD367, and SD369 enhancers (Figures 1E–1G) in which the transcript levels of UPF1 and other NMD components remained unchanged (Figure 7H). Thus, enhancing PVX-GFP virulence did not overtly compromise the integrity of the NMD machinery. However, the RNA steady-state levels of known *Arabidopsis* NMD targets were consistently increased in the four enhancers in a manner paralleling the PVX-GFP levels (Figures 7H and 7I). Therefore, virulent PVX-GFP infection, restricted by NMD in the *dcl4* background (Figure 3D), concomitantly reduces endogenous NMD activity, suggesting that PVX either encodes a dedicated NMD suppressor protein or promotes a cellular state unfavorable to this pathway.

DISCUSSION

The Values of Sensitized Genetic Screens

Our use of the *rdr6*-sensitized background enabled the recovery of many missense alleles of primary silencing factors in *Arabidopsis*. The ongoing characterization of additional PVX-GFP enhancers may thus identify additional and perhaps specific components of this pathway, still genetically poorly characterized in plants and metazoans. The sensitized screen also uncovered *upf1* as a silencing-unrelated PVX-GFP enhancer mutation. Using all available *NMD* mutants of *Arabidopsis* and natural infection settings further established this posttranscriptional RNA quality control pathway as a general bottleneck to RNA virus infection. A second merit of the *rdr6*-sensitized screen was the recovery of suppressor mutations. Given the striking replicase bias of intragenic mutations, additional and as yet uncharacterized suppressors are likely to affect host-encoded factors required for PVX replication. For most plant viruses, such factors have remained elusive because large-scale infection procedures required for their identification have proven extremely labor-intensive, as illustrated by studies of tobamo- and potyvirus compatibility in *Arabidopsis* (Ishikawa et al., 1991; Lellis et al., 2002). Consequently, genetic investigations of plant-RNA virus interactions have been mostly conducted in yeast, where replication of RNA viruses was reconstructed and enhancer/suppressor mutations recovered (Kushner et al., 2003; Panavas et al., 2005). The *Arabidopsis rdr6* PVX-GFP system holds, therefore, credible promises for the in planta identification of original host-encoded replication components.

NMD as a General Outcome of Virus Infections

Subgenomic RNAs allow compacting more genetic information into a shorter genome, a conundrum faced by all viruses. Using dedicated sgRNA promoters, viruses can thereby regulate the timing and levels of various proteins produced from a single polycistronic RNA. However, we show here that a major downside to sgRNA production is to bring gRNAs into an NMD-promoting context by creating an extended 3′ UTR downstream of the first ORF, usually encoding the viral replicase or one of its cofactors. Given that NMD and its modes of activation are conserved across kingdoms, this host RNA quality control pathway is likely to intercept many viruses in the alpha-like and carmo-like superfamilies that include most sgRNA-producing viruses. Supporting this idea, a recent genome-wide RNAi screen conducted in human cells has identified NMD as a major restriction hub for the *Semliki forest alphavirus* (SFV; G. Ballistreri and A. Helenius, personal communication). Our study of PVX further illustrates how multiple 3′-coterminal sgRNAs may also engage the host NMD machinery, resulting in their reduced stability. A notable exception is the 3′-most terminal sgRNA, which is naturally devoid of iTC. Viruses with large RNA genomes such as plant *Closteroviridae* or animal *Nidovirales* may produce up to nine sgRNAs altogether and are thus expected to be strongly restricted by NMD. Added to the long 3′ UTR configuration of the TCV P28/88 ORFs, readthrough translation of the P88 viral replicase could explain the strong impact of NMD on the TCV gRNA levels (Figure 7A). Moreover, a small uORF created in sgRNA2 by the 3′ overlapping end of the P9 ORF may further specifically limit the expression of P38 in an NMD-dependent manner (Figures 7A and S2). In line with work conducted in yeast with IRES-containing mRNAs (Holbrook et al., 2006), the TCV experiments also suggest that 5′-cap and 3′-polyA tail are dispensable for viral RNAs to engage the NMD machinery, reinforcing the notion that this host RNA quality control pathway will intercept a broad range of viruses.

NMD, RNA Silencing, and the Evolution of Viral Genomes

From the analyses conducted here with PVX, we infer that NMD might be triggered during the first rounds of gRNA translation, required for replicase production. This should precede the onset of antiviral silencing, because a sufficient build-up in viral replicase would be required for dsRNA RIs to accumulate and stimulate host Dicers. Not replicated, sgRNAs are also less likely to contribute to primary RNA silencing, whereas they are fully sensitive to NMD. Thus, the two pathways might be largely disconnected in early infection, agreeing with their nonepistatic interaction. However, as the infection progresses, secondary RNA silencing via host-encoded RDRs is likely to affect the same RNA pool as the one controlled by NMD. Competition for substrates could explain why viral GFP accumulation was higher in *rdr6 upf1* double mutants than was expected from the additive effects of each mutation (Figure 3C). Also consistent with a competition at the level of silencing amplification, deficiencies in RNA quality control, including NMD, enhance

RDR6-dependent transgene silencing in *Arabidopsis* (Moreno et al., 2013). In effect, saturation of NMD by increasing amounts of viral RNAs may constitute a switch for RDR action and secondary RNA silencing during infections.

RNA silencing and NMD share superficial similarities in that they are both activated by intrinsic and distinctive features of viral RNA: the double-strandedness of RIs for the former, and the presence of iTCs and extended 3′ UTRs for the latter. The two pathways also have major endogenous gene regulation and genome integrity functions, and both are broadly conserved across all kingdoms of life, such that it remains unclear if defensive as opposed to regulatory functions have primarily driven their emergence during evolution. Nonetheless, crucial differences also set these two RNA-based restriction pathways apart. First, while RIs are an essential and unavoidable component of RNA virus biology, many NMD-activating features of translated RNAs can be circumvented by viruses (see below). Second, RNA silencing is both nondiscriminative and *trans*-active, since virus-derived siRNAs may target any type of complementary viral RNA; NMD, by contrast, only affects specific RNA substrates in *cis*. Thus, while RNA silencing undoubtedly defines an intrinsic immunity against most, if not all RNA viruses, the effects of NMD as a host RNA quality control mechanism probably entail a much more graded spectrum of outcomes during virus infections. At one end of this spectrum, NMD probably acts as a potent restriction pathway against viruses, which, like TCV, display NMD-activating features that significantly impede production of the viral replicase. The other end of the spectrum is epitomized by potyviruses and their large polyprotein, which, although suboptimal for the control of individual viral products, intrinsically allows these viruses to evade NMD entirely. Combined with their ability to efficiently suppress RNA silencing via HcPro, this might explain the success of potyviruses, which account for ~30% of all known plant viruses (Hull, 2001).

Between the two ends of the spectrum probably lie many situations, including some where viruses might have evolved to reduce the primary impact of NMD on their core replication machinery and to simultaneously usurp this pathway for specific regulatory purposes. This idea might be illustrated with the tripartite BMV genome, whose two-component replicase functions are each encoded by a separate monocistronic RNA precluding the effects of NMD altogether; the bicistronic RNA3, by contrast, puts the 5′-terminal ORF of the movement protein into an NMD-favorable context that might allow fine-tuning of its expression during the complex process of cell-to-cell virus spread (Hull, 2001). Likewise, the differential expression of the geminiviral AL2 and AL3 proteins from a polycistronic RNA is permitted by a highly conserved uORF, suggesting that DNA viruses might also exploit NMD as a posttranscriptional RNA regulation mechanism (Shung and Sunter, 2009). Altogether, both the viral restriction and the proposed regulatory effects of NMD are likely to dynamically shape viral genomes and their various modes of expression, a notion with strong implications for the origins and evolution of these pathogens.

Defense, Counter-Defense, and Counter-Counter-Defense?

The constraints imposed upon viruses that are unable to evade, or adapt to, NMD might be strong enough to instigate the elaboration, by these pathogens, of dedicated inhibitory mechanisms. This idea is substantiated by previous findings made with mammalian retroviruses, whose mRNAs were noted to present characteristics uncommonly found in host cell transcripts, including long 3′ UTRs, retained introns, and multiple ORFs, which are all known triggers of NMD (Withers and Beemon, 2010). Accordingly, experimental evidence suggests that proteins of the human-T cell leukemia virus (HTLV-1) protect viral mRNAs from the detrimental action of NMD, collaterally causing misregulation of endogenous NMD targets (Mocquet et al., 2012; Nakano et al., 2013); a specific *cis*-element called Rous sarcoma virus (RSV) stability element also appears to protect the RSV genomic RNA against host NMD (Withers and Beemon, 2010). Work conducted in parallel to the present study further extends the above findings with retroviruses to (+)strand RNA viruses by demonstrating how the SFV-encoded NSP3 protein suppresses NMD targeted against this virus in human cells (G. Ballistreri and A. Helenius, personal communication). The virulence of plant (+)strand RNA viruses is also possibly underpinned by their ability to suppress NMD in addition to RNA silencing. Indeed, *Arabidopsis* with a *DCL4*-deficient but *UPF1*-proficient background displayed enhanced PVX accumulation coinciding with high levels of known *Arabidopsis* NMD targets (Figure 7H). More work is now required to identify which factor(s), among the PVX-encoded proteins, might interfere with NMD, although these effects could equally result from the mere titration of the host NMD machinery by highly abundant viral substrates.

Whether based on active suppression, titration, or other mechanisms, this virus-induced release of endogenous NMD might be relevant in the context of host counter-counter-defense responses to the perturbation of basal resistance by pathogens. Indeed, the vegetative growth anomalies of NMD-deficient *Arabidopsis*, which correlate with increased resistance against biotrophes, are suppressed by secondary mutations affecting salicylic acid (SA) signaling (Riehs-Kearnan et al., 2012). The constitutive SA signaling and defense activation in NMD mutants is largely contributed by the upregulation of a class of *R* genes normally maintained at a low expression level by NMD (J. Gloggnitzer and K. Riha, personal communication). NMD suppression by pathogens would thus in turn increase *R* gene expression and, consequently, elevate plant basal resistance. Remarkably, a near-identical molecular wiring has been described for a *R* gene class constitutively downregulated posttranscriptionally by endogenous siRNAs; pathogen-mediated suppression of silencing in that case would also lead to enhanced basal resistance (Shivaprasad et al., 2012). These findings unravel an unexpected degree of intricacy and complementarity between two unrelated RNA-based pathways. More generally, they implicate NMD as a strong bottleneck to RNA virus infections in plants and across kingdoms.

EXPERIMENTAL PROCEDURES

Plant Material

A. thaliana WT PVX-GFP and the parental line of the screen, sde1-1 PVX-GFP (otherwise referred to as *rdr6*), are both in the C24 ecotype (Dalmay et al., 2000b; Garcia et al., 2012). Mutants *upf1-5* (SALK_112922), *smg7-1* (SALK_073354), and *upf3-2* (SALK_097931) were previously described (Riehs-Kearnan et al., 2012). Genotyping primers are listed in Table S3.

Transient Expression Assays

Agrobacterium-mediated transient expression and infections in *N. benthamiana* were as described (Voinnet et al., 2003). The transient NMD inactivation assay using the dominant-negative version of UPF1 was previously described (Kertész et al., 2006).

Viral Strains

The plasmids expressing PVX-GFP, PVX-GFPΔCP, TuMV-GFP, and TCV were previously described (Lellis et al., 2002; Azevedo et al., 2010). PVX-GFP, TCV, and TuMV-GFP sap were prepared by grinding 0.5 g of *N. benthamiana* leaves transiently expressing the corresponding constructs in 1.5 ml KH_2PO_4 0.1 M at pH 7.4 and inoculating 20 μl of sap per leaves. Leaves were observed and harvested between 3 and 7 dpi.

Mutant Mapping

Mutant mapping was conducted on individual segregants selected in F2 populations from a cross of our mutant lines in the *sde1-1* mutant background and C24 ecotype with the *rdr6-12* allele in the Columbia ecotype in order to maintain a constant *rdr6* mutant background. Polymorphic molecular markers between the C24 and Columbia ecotypes cited in the text are referenced in Table S3.

Molecular Cloning

The PVX-GFPΔa and a fragment corresponding to sgRNA3 (GFP-CP) were amplified from genomic DNA of the parental line (PL) with High-Fidelity Mastermix Phusion Taq polymerase (Finnzyme) with primers detailed in Table S3 and cloned in appropriate binary vectors for transient expression, pFGC5941, and pBIN61.

RNA Analysis

Total RNA was extracted from frozen tissues with Tri-Reagent (Sigma). High-molecular-weight and low-molecular-weight RNA analyses were conducted on 5 and 10–25 μg total RNA, respectively. RNA hybridization signals were quantified using the ImageJ software. For real-time RT-PCR analyses, total RNA was extracted with Rneasy Plant Mini Kit (QIAGEN). RNA samples were reverse-transcribed into cDNA using SuperScript III reverse transcriptase (Invitrogen) with a mix of oligo(dT) and random hexamers. The cDNA was quantified using a SYBR Green qPCR kit (Eurogentec) and gene-specific primers. PCR was performed in 384-well optical reaction plates heated for 10 min at 95°C, followed by 45 cycles of denaturation for 15 s at 95°C, annealing for 20 s at 60°C, and elongation for 40 s at 72°C. A melting curve was performed at the end of the amplification by steps of 1°C (from 95°C to 50°C). Transcript levels were normalized to that of Actin2.

Protein Extraction and Analysis

Total protein extracts were produced by direct tissue grinding in 8 M urea and resolved on SDS-PAGE. After electroblotting proteins on Immobilon-P membrane (Millipore), protein blot analysis was performed using antiserum to GFP at a dilution of 1/30,000, antiserum to PVX CP at a dilution of 1/5,000, and antiserum to TCV P38 at a dilution of 1/50,000 to 1/200,000.

Antibodies

Rabbit antisera were raised against immunogenic peptides identified on the PVX coat protein (MPKEGLIRPPSEAEM and KITKARAQSNDFASL) and affinity purified following the Double X protocol of Eurogentec SA.

SUPPLEMENTAL INFORMATION

Supplemental Information includes two figures and three tables and can be found with this article online at http://dx.doi.org/10.1016/j.chom.2014.08.001.

ACKNOWLEDGMENTS

This work was supported by the Bettencourt-Schueller foundation, the Agence Nationale pour la Recherche (ANR-10-LABX-0036_NETRNA) and by the NCCR "RNA & Disease" funded by the Swiss National Science Foundation. We thank Daniel Silhavy for kindly providing the binary vectors to perform the transient NMD inactivation assay and Peter Moffet for sending the PVX-GFP binary vector.

Received: February 17, 2014
Revised: April 16, 2014
Accepted: July 14, 2014
Published: August 21, 2014

REFERENCES

Azevedo, J., Garcia, D., Pontier, D., Ohnesorge, S., Yu, A., Garcia, S., Braun, L., Bergdoll, M., Hakimi, M.A., Lagrange, T., and Voinnet, O. (2010). Argonaute quenching and global changes in Dicer homeostasis caused by a pathogen-encoded GW repeat protein. Genes Dev. *24*, 904–915.

Boutet, S., Vazquez, F., Liu, J., Béclin, C., Fagard, M., Gratias, A., Morel, J.B., Crété, P., Chen, X., and Vaucheret, H. (2003). Arabidopsis HEN1: a genetic link between endogenous miRNA controlling development and siRNA controlling transgene silencing and virus resistance. Curr. Biol. *13*, 843–848.

Dalmay, T., Hamilton, A., Mueller, E., and Baulcombe, D.C. (2000a). Potato virus X amplicons in arabidopsis mediate genetic and epigenetic gene silencing. Plant Cell *12*, 369–379.

Dalmay, T., Hamilton, A., Rudd, S., Angell, S., and Baulcombe, D.C. (2000b). An RNA-dependent RNA polymerase gene in Arabidopsis is required for posttranscriptional gene silencing mediated by a transgene but not by a virus. Cell *101*, 543–553.

Dalmay, T., Horsefield, R., Braunstein, T.H., and Baulcombe, D.C. (2001). SDE3 encodes an RNA helicase required for post-transcriptional gene silencing in Arabidopsis. EMBO J. *20*, 2069–2078.

Deleris, A., Gallego-Bartolome, J., Bao, J., Kasschau, K.D., Carrington, J.C., and Voinnet, O. (2006). Hierarchical action and inhibition of plant Dicer-like proteins in antiviral defense. Science *313*, 68–71.

Ding, S.W., and Voinnet, O. (2007). Antiviral immunity directed by small RNAs. Cell *130*, 413–426.

Garcia, D., Garcia, S., Pontier, D., Marchais, A., Renou, J.P., Lagrange, T., and Voinnet, O. (2012). Ago hook and RNA helicase motifs underpin dual roles for SDE3 in antiviral defense and silencing of nonconserved intergenic regions. Mol. Cell *48*, 109–120.

Hemenway, C., Weiss, J., O'Connell, K., and Tumer, N.E. (1990). Characterization of infectious transcripts from a potato virus X cDNA clone. Virology *175*, 365–371.

Herr, A.J., Jensen, M.B., Dalmay, T., and Baulcombe, D.C. (2005). RNA polymerase IV directs silencing of endogenous DNA. Science *308*, 118–120.

Holbrook, J.A., Neu-Yilik, G., Gehring, N.H., Kulozik, A.E., and Hentze, M.W. (2006). Internal ribosome entry sequence-mediated translation initiation triggers nonsense-mediated decay. EMBO Rep. *7*, 722–726.

Hull, R. (2001). Matthews' Plant Virology, Fourth Edition. (London: Academic Press).

Ishikawa, M., Obata, F., Kumagai, T., and Ohno, T. (1991). Isolation of mutants of Arabidopsis thaliana in which accumulation of tobacco mosaic virus coat protein is reduced to low levels. Mol. Gen. Genet. *230*, 33–38.

Isken, O., Kim, Y.K., Hosoda, N., Mayeur, G.L., Hershey, J.W., and Maquat, L.E. (2008). Upf1 phosphorylation triggers translational repression during nonsense-mediated mRNA decay. Cell *133*, 314–327.

Kalyna, M., Simpson, C.G., Syed, N.H., Lewandowska, D., Marquez, Y., Kusenda, B., Marshall, J., Fuller, J., Cardle, L., McNicol, J., et al. (2012). Alternative splicing and nonsense-mediated decay modulate expression of important regulatory genes in Arabidopsis. Nucleic Acids Res. *40*, 2454–2469.

Kerényi, Z., Mérai, Z., Hiripi, L., Benkovics, A., Gyula, P., Lacomme, C., Barta, E., Nagy, F., and Silhavy, D. (2008). Inter-kingdom conservation of mechanism of nonsense-mediated mRNA decay. EMBO J. *27*, 1585–1595.

Kertész, S., Kerényi, Z., Mérai, Z., Bartos, I., Pálfy, T., Barta, E., and Silhavy, D. (2006). Both introns and long 3′-UTRs operate ascis-acting elements to trigger nonsense-mediated decay in plants. Nucleic Acids Res. *34*, 6147–6157.

Kervestin, S., and Jacobson, A. (2012). NMD: a multifaceted response to premature translational termination. Nat. Rev. Mol. Cell Biol. *13*, 700–712.

Kushner, D.B., Lindenbach, B.D., Grdzelishvili, V.Z., Noueiry, A.O., Paul, S.M., and Ahlquist, P. (2003). Systematic, genome-wide identification of host genes

affecting replication of a positive-strand RNA virus. Proc. Natl. Acad. Sci. USA *100*, 15764–15769.

Le Hir, H., Gatfield, D., Izaurralde, E., and Moore, M.J. (2001). The exon-exon junction complex provides a binding platform for factors involved in mRNA export and nonsense-mediated mRNA decay. EMBO J. *20*, 4987–4997.

Lellis, A.D., Kasschau, K.D., Whitham, S.A., and Carrington, J.C. (2002). Loss-of-susceptibility mutants of Arabidopsis thaliana reveal an essential role for eIF(iso)4E during potyvirus infection. Curr. Biol. *12*, 1046–1051.

Li, J., Yang, Z., Yu, B., Liu, J., and Chen, X. (2005). Methylation protects miRNAs and siRNAs from a 3′-end uridylation activity in Arabidopsis. Curr. Biol. *15*, 1501–1507.

Mocquet, V., Neusiedler, J., Rende, F., Cluet, D., Robin, J.P., Terme, J.M., Duc Dodon, M., Wittmann, J., Morris, C., Le Hir, H., et al. (2012). The human T-lymphotropic virus type 1 tax protein inhibits nonsense-mediated mRNA decay by interacting with INT6/EIF3E and UPF1. J. Virol. *86*, 7530–7543.

Moreno, A.B., Martínez de Alba, A.E., Bardou, F., Crespi, M.D., Vaucheret, H., Maizel, A., and Mallory, A.C. (2013). Cytoplasmic and nuclear quality control and turnover of single-stranded RNA modulate post-transcriptional gene silencing in plants. Nucleic Acids Res. *41*, 4699–4708.

Muhlrad, D., and Parker, R. (1999). Recognition of yeast mRNAs as "nonsense containing" leads to both inhibition of mRNA translation and mRNA degradation: implications for the control of mRNA decapping. Mol. Biol. Cell *10*, 3971–3978.

Nagy, P.D., and Pogany, J. (2012). The dependence of viral RNA replication on co-opted host factors. Nat. Rev. Microbiol. *10*, 137–149.

Nakano, K., Ando, T., Yamagishi, M., Yokoyama, K., Ishida, T., Ohsugi, T., Tanaka, Y., Brighty, D.W., and Watanabe, T. (2013). Viral interference with host mRNA surveillance, the nonsense-mediated mRNA decay (NMD) pathway, through a new function of HTLV-1 Rex: implications for retroviral replication. Microbes Infect. *15*, 491–505.

Panavas, T., Serviene, E., Brasher, J., and Nagy, P.D. (2005). Yeast genome-wide screen reveals dissimilar sets of host genes affecting replication of RNA viruses. Proc. Natl. Acad. Sci. USA *102*, 7326–7331.

Pumplin, N., and Voinnet, O. (2013). RNA silencing suppression by plant pathogens: defence, counter-defence and counter-counter-defence. Nat. Rev. Microbiol. *11*, 745–760.

Rayson, S., Arciga-Reyes, L., Wootton, L., De Torres Zabala, M., Truman, W., Graham, N., Grant, M., and Davies, B. (2012). A role for nonsense-mediated mRNA decay in plants: pathogen responses are induced in Arabidopsis thaliana NMD mutants. PLoS ONE *7*, e31917.

Riehs-Kearnan, N., Gloggnitzer, J., Dekrout, B., Jonak, C., and Riha, K. (2012). Aberrant growth and lethality of Arabidopsis deficient in nonsense-mediated RNA decay factors is caused by autoimmune-like response. Nucleic Acids Res. *40*, 5615–5624.

Shivaprasad, P.V., Chen, H.M., Patel, K., Bond, D.M., Santos, B.A., and Baulcombe, D.C. (2012). A microRNA superfamily regulates nucleotide binding site-leucine-rich repeats and other mRNAs. Plant Cell *24*, 859–874.

Shung, C.Y., and Sunter, G. (2009). Regulation of Tomato golden mosaic virus AL2 and AL3 gene expression by a conserved upstream open reading frame. Virology *383*, 310–318.

Soosaar, J.L., Burch-Smith, T.M., and Dinesh-Kumar, S.P. (2005). Mechanisms of plant resistance to viruses. Nat. Rev. Microbiol. *3*, 789–798.

Voinnet, O., Rivas, S., Mestre, P., and Baulcombe, D. (2003). An enhanced transient expression system in plants based on suppression of gene silencing by the p19 protein of tomato bushy stunt virus. Plant J. *33*, 949–956.

Withers, J.B., and Beemon, K.L. (2010). Structural features in the Rous sarcoma virus RNA stability element are necessary for sensing the correct termination codon. Retrovirology *7*, 65.